

# A unified theory for the cuprates, iron-based and similar superconducting systems: non-Fermi-liquid to Fermi-liquid crossover, low-energy and waterfall anomalies

J. Ashkenazi\*

*Physics Department, University of Miami,  
P.O. Box 248046, Coral Gables, FL 33124, U.S.A.*

(Dated: November 6, 2018)

A unified theory is outlined for the cuprates, Fe-based, and related superconductors. Their low-energy excitations are approached in terms of auxiliary particles representing combinations of atomic-like electron configurations, and the introduction of a Lagrange Bose field enables their treatment as bosons or fermions. This theory correctly describes the observed phase diagram of the cuprates, including the non-Fermi-liquid to FL crossover in the normal state, the existence of Fermi arcs below  $T^*$  and of “marginal-FL” behavior above it. The anomalous behavior of numerous physical quantities is accounted for, including kink- and waterfall-like spectral features, the drop in the scattering rates below  $T^*$  and more radically below  $T_c$ , and an effective increase in the density of carriers with  $T$  and  $\omega$ , reflected in transport, optical and other properties. Also is explained the correspondence between  $T_c$ , the resonance-mode energy, and the increase in the gap below  $T_c$ .

PACS numbers: 71.10.Hf, 71.10.Li, 71.10.Pm, 74.20.-z, 74.20.Mn, 74.20.Rp, 74.25.Dw, 74.25.Jb, 74.72.-h

High- $T_c$  superconductivity (SC) has been in the forefront of condensed-matter physics research since its discovery in the cuprates over 22 years ago. This system is characterized by anomalous behavior of many of its physical properties [1, 2, 3, 4, 5, 6, 7, 8, 9] which led to the suggestion of non-Fermi-liquid (non-FL) models [10, 11]. The recent discovery of Fe-based high- $T_c$  SCs (referred to below as FeSCs) provides a new test case for high- $T_c$  theories, especially in view of the striking similarity of their anomalous properties to those of the cuprates (see Ref. [12]).

Recently [12], a unified theory for the cuprates and the FeSCs has been derived by the author on the basis of common features in their electronic structures, including quasi-two-dimensionality, and the large- $U$  nature of the low-energy electron orbitals. A Hamiltonian,  $\mathcal{H}$ , has been written down [12], where such electrons are approached in terms of auxiliary particles [13], representing combinations of atomic-like electron configurations, and a Lagrange field maintaining a constraint imposed on them.

The auxiliary particles consist of [12]: (i) boson “svivons” which represent configurations of the undoped “parent” compounds, and their condensation results in static or dynamical inhomogeneities, and consequently in a resonance mode (RM); (ii) fermion “quasi-electrons” (QEs) which represent configurations with an excess of an electron or a hole over those of the parent compounds, and their dynamics determines charge transport; (iii) boson “lagrons” of the constraint Lagrange field which represents an effective fluctuating potential, enabling the treatment of svivons and QEs as bosons and fermions.

Within a one-orbital model for the hole-doped cuprates [10] a svivon state of spin  $\sigma$  ( $=\uparrow$  or  $\downarrow$ ) at site  $i$  is created by  $s_{i\sigma}^\dagger$ , and a QE state is created by  $q_i^\dagger \equiv h_i$ , where  $h_i^\dagger$  creates a Zhang-Rice singlet.  $\mathcal{H}$  [12] is expressed in terms

of the auxiliary-particle operators and parameters determined in first-principles calculations by few groups (see Ref. [12]). The set of parameters used is:  $t = 0.43$  eV,  $t' = -0.07$  eV,  $t'' = 0.03$  eV, and  $J = 0.1$  eV. Unlike in RVB models [10], the condensation-induced inhomogeneities result here in a multi-component scenario.

The svivon and QE Green’s functions (GF) consist of “normal” and (within their condensates) “anomalous” terms, based on  $\langle s_{i\sigma} s_{j\sigma}^\dagger \rangle$  and  $\langle q_i q_j^\dagger \rangle$ , or  $\langle s_{i\uparrow} s_{j\downarrow} \rangle$  and  $\langle q_i q_j \rangle$ , respectively. The creation operator of an electron is expressed as [12]:  $d_{i\sigma}^\dagger \cong s_{i\sigma}^\dagger q_i^\dagger$ , and, thus, the normal (anomalous) electron GF could be diagrammatically presented, at the zeroth-order, as a convolution of bubble diagrams of normal (anomalous) QE and svivon GF. Let us denote the matrix of these approximate electron GF by  $\underline{\mathcal{G}}_0(\underline{\mathcal{E}}_0)$ ; it is diagonal in the  $\mathbf{k}$  representation.  $\mathcal{H}$  [12] introduces to  $\underline{\mathcal{G}}_0(\underline{\mathcal{E}}_0)$  self-energy corrections due to multiple scattering of QE-svivon pairs.

For un-paired QEs, the corrections to  $\underline{\mathcal{G}}_0$  can be expressed as a sum of a geometrical series in powers of  $\underline{\mathcal{G}}_0 \underline{t}$  (where the matrix  $\underline{t}$  consists of the transfer and intra-site terms in  $\mathcal{H}$ ), yielding  $(\underline{1} - \underline{\mathcal{G}}_0 \underline{t})^{-1}$ . Using Dyson’s equation, the normal electron GF matrix is expressed as:

$$\underline{\mathcal{G}} = \underline{\mathcal{G}}_0 (\underline{1} - 2\underline{\mathcal{G}}_0 \underline{t})^{-1} (\underline{1} - \underline{\mathcal{G}}_0 \underline{t}). \quad (1)$$

Thus, there are two types of poles in  $\underline{\mathcal{G}}$ ; while  $\underline{\mathcal{G}}_0$  contributes a non-FL distribution of convoluted QE-svivon poles,  $(\underline{1} - 2\underline{\mathcal{G}}_0 \underline{t})^{-1}$  introduces FL-like electron poles. Indeed, the phase diagram of the cuprates [14] indicates a non-FL to FL crossover between the underdoped and the overdoped normal-state regimes [1, 9].

The auxiliary-particle spectra are evaluated through a self-consistent second-order diagrammatic expansion [12]. The lagrons are soft at wave vectors corresponding to major spin and charge fluctuations (where an in-

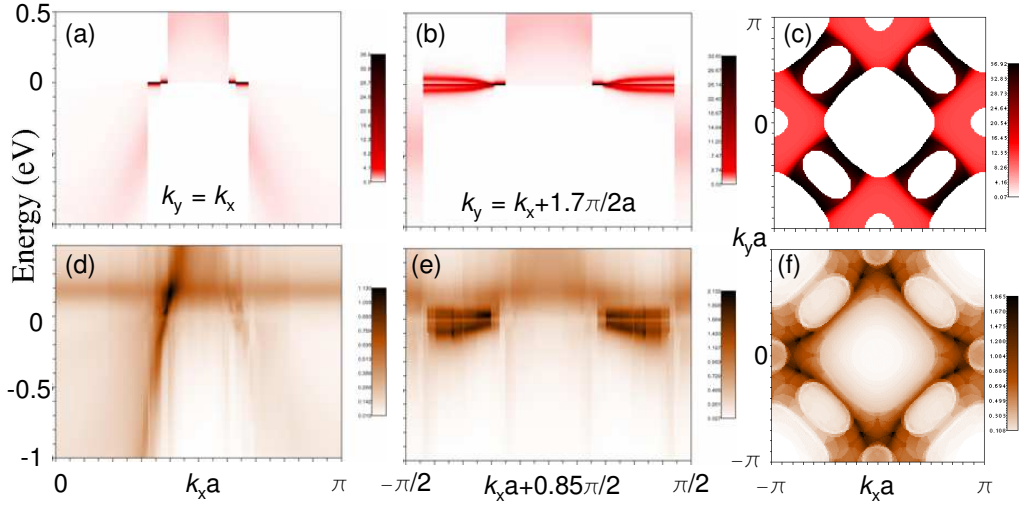


FIG. 1: The QE (a-c) and electron (d-f) spectral functions in optimally hole-doped cuprates along a “line of nodes” (a,d), along a parallel line (b,e) shifted by  $0.425\pi(\hat{y} - \hat{x})$ , and on the “Fermi surface” (c,f), determined at  $\omega = -0.1k_B T$ .

homogeneous enforcement of the constraint is essential). Consequently, their energy band  $\omega^\lambda(\mathbf{q})$  is characterized [12] by four V-shape minima  $\ll k_B T$  at  $\mathbf{Q}_m = \mathbf{Q} + \delta\mathbf{q}_m$ , where  $\mathbf{Q} = \frac{\pi}{a}(\hat{x} + \hat{y})$  is the parent-compound’s antiferromagnetic (AF) wave vector, and  $\delta\mathbf{q}_m = \pm\delta q\hat{x}$  or  $\pm\delta q\hat{y}$  are modulations corresponding to striped structures (typically  $\delta q \cong \pi/4a$ ). Degenerate svivon condensates are obtained [12], with energy minima at  $\pm\mathbf{Q}_m/2$ , and in the absence of symmetry-breaking long-range order, the system is in a combination of these states.

The QE spectrum is evaluated treating the fluctuations between the combined svivon condensates adiabatically. By introducing appropriate phase factors to the QE and svivon states, their  $\mathbf{k}$  values are shifted by  $\mathbf{Q}/2$  or  $-\mathbf{Q}/2$ , resulting in a correspondence between the QE and electron Brillouin zones (BZs). The evaluated QE spectral functions for hole-doped cuprates, at an optimal stoichiometry (corresponding to  $n^s \equiv \langle s_{i\sigma}^\dagger s_{i\sigma} \rangle = 0.42$ ), within the “hump phase” [14] ( $k_B T = 0.01$  eV), are presented in Fig. 1(a-c). The QE spectrum has a “bare” and a “dressed” part, due to coupling to svivon fluctuations and lagrons [12]. The bare part is independent of  $t$ , and determined by [12]  $\bar{t}' = t' + 4n^s J$  and  $\bar{t}'' = t'' + 2n^s J$ , resulting in *equivalent* “main” and “shadow” QE bands.

The electron spectral functions, obtained on the basis of Eq. (1), and the QE and svivon [12] spectra in this phase, are presented in Fig. 1(d-f). The high-weight of the svivon poles around their (averaged) minimal energies results in band-like features in the electron spectrum which follow the QE band. The FL-like electron poles in Eq. (1) break the equivalence between the main and shadow bands, in agreement with experiment [15, 16].

Coupling of QEs to svivon fluctuations [12] depends on  $t$ , and introduces shifts in their energies towards zero. This results in BZ areas of low-energy “flat” QE bands and apparent discontinuities to areas of higher energies

(see Fig. 1(a-b)). These features are modified in the electron spectrum (see Fig. 1(d-e)) to the observed [17] low-energy kinks and waterfall-like features above them.

The low-energy QE and svivon spectra are strongly renormalized by their coupling to lagrons (through coefficients  $\gamma(\mathbf{q})$ ). The resulting QE self-energy corrections (to  $\epsilon_0^q(\mathbf{k})$ ) are expressed, for un-paired QEs, as:

$$\Sigma^q(\mathbf{k}, z) \cong \frac{1}{N} \sum_{\mathbf{q}} |\gamma(\mathbf{q})|^2 \int d\omega^q A^q(\mathbf{k} - \mathbf{q}, \omega^q) \times \left[ \frac{b_T(\omega^\lambda(\mathbf{q})) + f_T(-\omega^q)}{z - \omega^\lambda(\mathbf{q}) - \omega^q} + \frac{b_T(\omega^\lambda(\mathbf{q})) + f_T(\omega^q)}{z + \omega^\lambda(\mathbf{q}) - \omega^q} \right], \text{ where} \quad (2)$$

$$A^q(\mathbf{k}, \omega) = \frac{\Gamma^q(\mathbf{k}, \omega)/2\pi}{[\omega - \epsilon_0^q(\mathbf{k}) - \Re\Sigma^q(\mathbf{k}, \omega)]^2 + [\frac{1}{2}\Gamma^q(\mathbf{k}, \omega)]^2} \quad (3)$$

are the QE spectral functions,  $\Gamma^q(\mathbf{k}, \omega)$  are their scattering rates, and  $b_T$  ( $f_T$ ) is the Bose (Fermi) distribution function. The low-energy  $\Sigma^q$  is dominated by the contribution of lagrons around their minima  $0 < \omega^\lambda(\mathbf{Q}_m) \ll k_B T$  (referred to below as “ $\mathbf{Q}_m$  lagrons”), and of those of energy  $\sim \omega^\lambda(\mathbf{Q})$  at their “extended saddle point” around  $\mathbf{Q}$  [12] (referred to below as “ $\mathbf{Q}$ -ESP lagrons”).

As can be seen in Fig. 1, low-energy QEs around the “nodal points”  $\pm\frac{\pi}{2}(\hat{x} \pm \hat{y})$  are not coupled to other low-energy QEs through  $\mathbf{Q}_m$  lagrons, and the spectral functions of such QEs (referred to as “arcons”) are characterized by a simple peak, as is sketched in Fig. 2(a). On the other hand, low-energy QEs around the “antinodal points”  $\pm\pi\hat{x}$  and  $\pm\pi\hat{y}$  are coupled to other low-energy QEs through  $\mathbf{Q}_m$  lagrons, resulting in the splitting of the spectral-function peaks of such QEs (due to the inhomogeneities) into positive- and negative-energy “humpons”. For dynamical inhomogeneities, a “stripon” peak remains

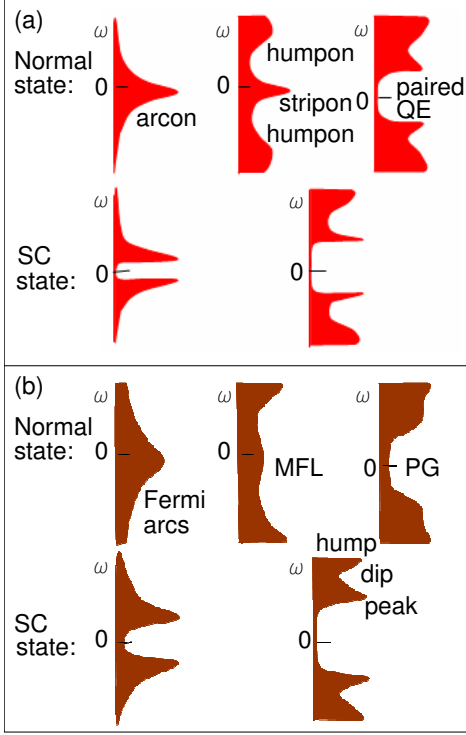


FIG. 2: Low-energy QE (a) and electron (b) spectral functions in the normal and SC states, close to the nodal (arcon, Fermi arcs) and antinodal (humpon, stripon, MFL, paired QE, PG, peak, dip, hump) points in hole-doped cuprates.

between the humpons, as is sketched in Fig. 2(a).

The humpon peaks are rather wide, while the width of the stripon peaks (see below), as well as their position relative to zero (determined by the effective QE chemical potential  $\mu - \lambda$  [12]), scale with  $T$ . The  $\mathbf{Q}$ -ESP lagrons maintain an energy separation  $> \omega^\lambda(\mathbf{Q})$  between the stripon and the two humpons. Analogous expressions to Eq. (2) are obtained for the normal and anomalous svivon self-energy corrections due to their coupling to lagrons. The effect of the  $\mathbf{Q}$ -ESP lagrons there is the stabilization of high-weight svivon states below  $\sim \omega^\lambda(\mathbf{Q})$ . Thus [12], the RM energy ( $E_{\text{RM}}$ ) is  $\sim \omega^\lambda(\mathbf{Q})$ .

Eq. (2) yields a peculiar behavior for  $\Gamma^q(\mathbf{k}, \omega) \equiv 2\Im\Sigma^q(\mathbf{k}, \omega - i0^+)$ . In the low  $\omega/T$  limit the dominant contribution to  $\Gamma^q$  (for stripions) is due to  $\mathbf{Q}_m$  lagrons; the integration of  $b_T(\omega^\lambda)$  yields for them a factor  $\propto T^2$  which is multiplied by a factor  $\propto 1/T$  due to the coupled-stripon spectral functions (see Eq. (3)), resulting in  $\Gamma^q(\mathbf{k}, \omega) \propto T$ . In the high  $\omega/T$  limit, the dominant contribution to  $\Gamma^q$  is due to the continuum of lagrons [12] where  $b_T(\omega^\lambda) + f_T(\omega^\lambda \pm \omega)$  is either  $\sim 1$  or  $\sim 0$ ; the  $\mathbf{q}$  summation in Eq. (2) then turns into an integration on the normalized  $A^q$ , resulting in  $\Gamma^q(\mathbf{k}, \omega) \propto \omega$ .

A similar behavior is obtained in this phase also for the svivon scattering rates  $\Gamma^s$ , through analogous expressions to Eq. (2). The electron scattering rates are deter-

mined through  $\underline{\mathcal{G}}$  (see Eq. (1)). Let  $\epsilon^q(\mathbf{k}_1) + \frac{1}{2}i\Gamma^q(\mathbf{k}_1)$  and  $\epsilon^s(\mathbf{k}_2) + \frac{1}{2}i\Gamma^s(\mathbf{k}_2)$  be poles of QE and svivon GF, respectively; the  $\mathbf{k} = \mathbf{k}_1 + \mathbf{k}_2$  element of  $\underline{\mathcal{G}}_0$  contributes to  $\underline{\mathcal{G}}$  a pole at  $\epsilon^q(\mathbf{k}_1) \pm \epsilon^s(\mathbf{k}_2) + \frac{1}{2}i[\Gamma^q(\mathbf{k}_1) + |\Gamma^s(\mathbf{k}_2)|]$ , with a weight scaling with  $b_T(\epsilon^s(\mathbf{k}_2) \pm \frac{1}{2}i\Gamma^s(\mathbf{k}_2)) + f_T(\mp(\epsilon^q(\mathbf{k}_1) + \frac{1}{2}i\Gamma^q(\mathbf{k}_1)))$ . (Different poles correspond to different arcs, stripions, humpons, as well as positive and negative svivon energies [12]). Thus, if the role of such convoluted poles is dominant in  $\underline{\mathcal{G}}$ , the electron scattering rates have a similar dependence on  $\omega$  and  $T$  as  $\Gamma^q$ , and this corresponds to a marginal-Fermi-liquid (MFL) phase [11].

The signature of the low-energy QE spectral peaks on the electron spectrum is sketched in Fig. 2(b). The convolution with svivons broadens the trace of the stripon peak in the MFL phase; however, since many quantities are expressed in terms of QE and svivon contributions, they can be sensitive to its small width. The  $T$  and  $\omega$  dependencies of quantities determined by the QEs are then characterized by three energy scales, and crossovers between them; at the lowest energies only stripions and arcons contribute, while the humpons play a role in higher energies, and the almost detached higher-energy QEs (see Fig. 1(a-b)) have an effect only at the highest energies.

Such a behavior is observed in the scaling of the  $T$ -dependence of numerous quantities [7] in the humpon energy. Also, an effective increase in the carriers density with  $T$  and  $\omega$  is observed through the Hall constant [2] and the optical conductivity [8]. The low- $T$  dependence of the thermoelectric power has been analyzed in terms of a “narrow-band model” [3] (consistently with the effect of stripions and arcons), and the growing contribution of humpons at higher  $T$  results in a peculiar behavior [4] used to determine the doping level. Non-FL behavior, associated with the QE Fermi surface (see Fig. 1(c)), appears [16] as being due to hole and electron pockets around the nodal and antinodal points, respectively.

QE pairing is approached adapting the Migdal-Eliashberg theory [18], and deriving  $2 \times 2$  self-energy matrices  $\underline{\Sigma}^q(\mathbf{k}, z) = \Sigma^q(\mathbf{k}, z)\mathcal{I}_3 + \Re\Phi^q(\mathbf{k}, z)\mathcal{I}_1 + \Im\Phi^q(\mathbf{k}, z)\mathcal{I}_2$ , where  $\mathcal{I}_1$ ,  $\mathcal{I}_2$  and  $\mathcal{I}_3$  are the Pauli matrices, and  $\Phi^q$  is the pairing order parameter. The diagonalization of  $\epsilon_0^q(\mathbf{k})\mathcal{I}_3 + \underline{\Sigma}^q(\mathbf{k}, z)$  yields Bogoliubov states created by  $q_+^{\dagger}(\mathbf{k}, z)$ , and  $q_-^{\dagger}(\mathbf{k}, z)$ . Dyson’s equation yields QE GF poles at  $z = \pm\epsilon_0^q(\mathbf{k}) + \Sigma_{\pm}^q(\mathbf{k}, z) = E_{\pm}^q(\mathbf{k}, z) + i \cos(2\xi_{\mathbf{k}}^q(z))\Im\Sigma^q(\mathbf{k}, z)$ , where  $E_{\pm}^q(\mathbf{k}, z) = \pm\{[\epsilon_0^q(\mathbf{k}) + \Re\Sigma^q(\mathbf{k}, z)]^2 + [\Re\Phi^q(\mathbf{k}, z)]^2\}^{\frac{1}{2}}$ , and  $\sin(2\xi_{\mathbf{k}}^q(z)) = \Re\Phi^q(\mathbf{k}, z)/E_+^q(\mathbf{k}, z)$ . The spectral functions  $A_{\pm}^q(\mathbf{k}, \omega)$  are derived through an equivalent expression to Eq. (3), replacing  $\epsilon_0^q(\mathbf{k}) + \Sigma^q(\mathbf{k}, \omega - i0^+)$  by  $\pm\epsilon_0^q(\mathbf{k}) + \Sigma_{\pm}^q(\mathbf{k}, \omega - i0^+)$ .  $\Sigma^q(\mathbf{k}, z)$  and  $\Phi^q(\mathbf{k}, z)$  are evaluated on the basis of similar expressions to Eq. (2), where  $A^q(\mathbf{k}-\mathbf{q}, \omega^q)$  is replaced by  $\cos^2(\xi_{\mathbf{k}-\mathbf{q}}^q(\omega^q))A_+^q(\mathbf{k}-\mathbf{q}, \omega^q) + \sin^2(\xi_{\mathbf{k}-\mathbf{q}}^q(\omega^q))A_-^q(\mathbf{k}-\mathbf{q}, \omega^q)$ , for  $\Sigma^q$ , and by  $\frac{1}{2}\sin(2\xi_{\mathbf{k}-\mathbf{q}}^q(\omega^q))[A_+^q(\mathbf{k}-\mathbf{q}, \omega^q) - A_-^q(\mathbf{k}-\mathbf{q}, \omega^q)]$ , for  $\Phi^q$ .

The derivation of low-energy  $\Sigma^q$  and  $\Phi^q$  is expressed in

terms of contributions due to coupling to peaks of QE-lagron states of energies  $\sim \omega^q \pm \omega^\lambda(\mathbf{Q}_m) \simeq \omega^q$ , at points  $\sim \mathbf{k} + \mathbf{Q}_m$ , and of energies  $\sim \omega^q + \text{sign}(\omega^q)\omega^\lambda(\mathbf{Q})$  at points  $\sim \mathbf{k} + \mathbf{Q}$ . The resulting nonzero  $\Re\Phi^q(\mathbf{k}, \omega)$  does not change its sign as a function of  $\omega$ , and reverses it (maintaining its magnitude) when  $\mathbf{k}$  is shifted by  $\mathbf{Q}$ , consistently with an approximate  $d_{x^2-y^2}$  pairing. The coupling of stripons and arcons to the above (both positive- and negative-energy) peaks helps stabilize a nonzero  $\Phi^q$ , while terms of opposite signs are introduced to  $\Sigma^q$ . Consequently, the effect of  $\Phi^q$  on the gap dominates.

Since QE coupling through  $\mathbf{Q}_m$  lagrons is maximal for stripons, pairing is strongest for them (note that unlike the coupling constants between electrons and acoustic phonons which vanish for  $\mathbf{q} \rightarrow 0$ ,  $\gamma(\mathbf{q})$  remain constant for  $\mathbf{q} \rightarrow \mathbf{Q}_m$ ). Consequently, there exists a temperature range  $T_c < T < T^*$ , where  $\Phi^q \neq 0$  for stripons and humpons, but *not* for arcons, and it corresponds to the pseudogap (PG) phase [14]. The stripon peaks then split into positive- and negative-energy ones, as is sketched in Fig. 2(a), and their signature on the electron spectrum in the PG phase, is sketched in Fig. 2(b). The opening of a stripon gap causes a large reduction of the scattering rates below those of the MFL phase for  $\omega$  below the gap energy, and much less above it, in agreement with experiment [1, 5]. A decrease in  $T$  ( $> T_c$ ) results in the transition of arcons into stripon-humpons which would include all the arcons if  $\delta\mathbf{q}_m$  were small enough (see Fig. 1(c)). In such a case, the extension of  $T^*$  ( $> T_c$ ) to zero would result in the reduction of the Fermi arcs into points [19].

SC occurs when  $\Phi^q \neq 0$  *also* for arcons which are not coupled to other QE's through  $\mathbf{Q}_m$  lagrons, and it is induced through the  $\mathbf{Q}$ -ESP lagrons. Since the energy difference involved is  $\sim \omega^\lambda(\mathbf{Q}) \simeq E_{\text{RM}}$  (see above), it scales with  $k_B T_c$ , with a factor  $\sim 5$  (see Ref. [12]), similarly to the ratio between the energy of the relevant phonons and  $k_B T_c$  in strong-coupling phonon-mediated SCs. Thus the arcon peaks which are not on the lines of nodes split below  $T_c$ , resulting in the modification of the gap structure which resembles [20] the ‘‘onset of a second energy gap’’, scaling with  $\omega^\lambda(\mathbf{Q}) \simeq E_{\text{RM}} \simeq 5k_B T_c$ .

The opening of an SC gap diminishes low-energy scattering of gap-edge QE states, resulting in sharp split stripon and arcon peaks below  $T_c$ , while the humpon peaks remain wide (see Fig. 2(a)). The signature of the split peaks on the electron spectrum in the SC phase is sketched in Fig. 2(b). Since the SC gap is almost complete, the scattering rates are radically reduced below  $T_c$  [5] for  $\omega$  below the gap energy, while the effect above it is small. This results also in small-linewidth low-energy svivons, and thus [12] in a sharp RM. Since (see above) the energy separation between the stripon and the humpon  $> \omega^\lambda(\mathbf{Q})$ , a dip appears [6] between the peak and the hump, at about  $\omega^\lambda(\mathbf{Q}) \simeq E_{\text{RM}}$  above it.

The values of  $\omega^\lambda(\mathbf{q})$  and  $\gamma(\mathbf{q})$  are determined through the condition that the same ‘‘constraint-susceptibility’’

(CS) [12] is obtained using either the svivon or the QE spectrum. A major feature of the CS, based on the svivon spectrum in the SC state, is [12] the existence of a peak around  $\mathbf{k} = 0$  at an energy  $\sim E_{\text{RM}}$ . When it is calculated using the QE spectrum, this CS peak represents some average of the QE SC gap, and contributions to it cancel out [12] at points where  $\cos(2\xi_{\mathbf{k}}^q(\omega^q)) = [\epsilon_0^q(\mathbf{k}) + \Re\Sigma^q(\mathbf{k}, \omega^q)]/E_+^q(\mathbf{k}, \omega^q) = 0$ . For stripons and arcons one has  $\epsilon_0^q(\mathbf{k}) + \Re\Sigma^q(\mathbf{k}, \omega^q) \simeq 0$  for  $\Phi^q = 0$  but *not* for  $\Phi^q \neq 0$ . In the case of stripons, the modification of  $\Sigma^q(\mathbf{k}, \omega^q)$  for  $\Phi^q \neq 0$  includes contributions of opposite signs, due to coupling to positive- and negative-energy stripons through  $\mathbf{Q}_m$  lagrons. Thus, fine tuning of  $\omega^\lambda(\mathbf{q})$  and  $\gamma(\mathbf{q})$  yields smaller  $\cos(2\xi_{\mathbf{k}}^q(\omega^q))$  values for stripons than for arcons, such that the low-energy CS peak around  $\mathbf{k} = 0$  corresponds to  $\sim E_{\text{RM}}$ , as is required.

In conclusion, a unified theory for the cuprates and related SCs, where the low-energy excitations are approached in terms of combinations of atomic-like electron configurations, and a Lagrange Bose field enables treating them as bosons or fermions, has been shown to resolve mysteries of the cuprates. This includes their observed phase diagram, non-FL to FL crossover, the existence of MFL behavior and a PG phase with Fermi arcs, kink- and waterfall-like spectral features, the drop in the scattering rates in the PG phase, and further in the SC phase, an effective increase in the density of carriers with  $T$  and  $\omega$ , the correspondence between  $T_c$ ,  $E_{\text{RM}}$ , and the increase in the gap below  $T_c$ , *etc.* Similar anomalies to those of the cuprates exist in the FeSCs, and a forthcoming paper will address *both* similarities and differences between them.

---

\* Electronic address: jashkenazi@miami.edu

- [1] H. Takagi, *et al*, *Phys. Rev. Lett.* **69**, 2975 (1992).
- [2] H. Y. Hwang, *et al*, *Phys. Rev. Lett.* **72**, 2636 (1994).
- [3] J. Genossar, *et al*, *Physica C* **157**, 320 (1989).
- [4] S. D. Obertelli, *et al*, *Phys. Rev. B* **46**, 14928 (1992).
- [5] A. V. Puchkov, *et al*, *J. Phys.: Cond. Mat.*, **8**, 10049 (1996).
- [6] J. F. Zasadzinski, *et al*, *Phys. Rev. Lett.* **87**, 067005 (2001).
- [7] H. G. Luo, *et al*, *Phys. Rev. B* **77**, 014529 (2008).
- [8] D. B. Tanner, *et al*, *Physica B* **244**, 1 (1998).
- [9] G. S. Boebinger, *et al*, *Phys. Rev. Lett.* **77**, 5417 (1996).
- [10] P. W. Anderson, *Phys. Rev. Lett.* **64**, 1839 (1990).
- [11] C. M. Varma, *et al*, *Phys. Rev. Lett.* **63**, 1996 (1989).
- [12] J. Ashkenazi, arXiv:0809.4237, *J. Supercond. Nov. Magn.* DOI: 10.1007/s10948-008-0370-8.
- [13] S. E. Barnes, *Adv. Phys.* **30**, 801-938 (1981).
- [14] T. Honma, and P. H. Hor, *Phys. Rev. B* **77**, 184520 (2008).
- [15] K. Nakayama, *et al*, *Phys. Rev. B* **74**, 054505 (2006).
- [16] J. Chang, *et al*, *New J. Phys.* **10**, 103016 (2008).
- [17] W. Meevasana, *et al*, *Phys. Rev. B* **77**, 104506 (2008).
- [18] D. J. Scalapino, *et al*, *Phys. Rev.* **148**, 263 (1966).
- [19] A. Kanigel, *et al*, *Nature Physics* **2**, 447 (2006).

[20] W. S. Lee, *et al*, *Nature* **450**, 81 (2007).